Probing semiconductivity in crystals of stable semiquinone radicals: organic salts of 5,6-dichloro-2,3-dicyanosemiquinone (DDQ) radical anion

Krešimir Molčanov*[a], Dietmar Stalke*[b], Ana Šantić[a], Serhiy Demeshko[b], Vladimir Stilinović[c], Zhongyu Mou[d], Miklos Kertesz[d], Biserka Kojić-Prodić[a]

a Ruđer Bošković Institute, Bijenička 54, Zagreb HR-10000, Croatia

b Institut für Anorgansiche Chemie, Universität Göttingen, Tammanstraβe 4, D-37077 Göttingen, Germany

c Department of Chemistry, Faculty of Science, University of Zagreb, Horvatovac 102a, Zagreb HR-10000, Croatia

d Department of Chemistry and Institute of Soft Matter, Georgetown University, 424 Regents Hall, Washington DC 20057-1227, USA. Department of Chemistry and Institute of Soft Matter, Georgetown University, 424 Regents Hall, Washington DC 20057-1227, USA.

e-mail: kmolcano@irb.hr, dstalke@chemie.uni-goettingen.de

Supplementary Information

S1 ORTEP drawings

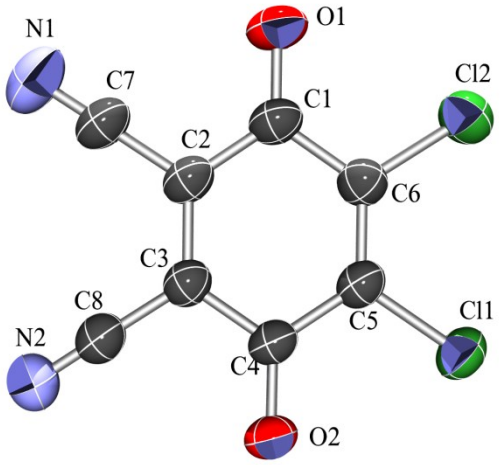

a)

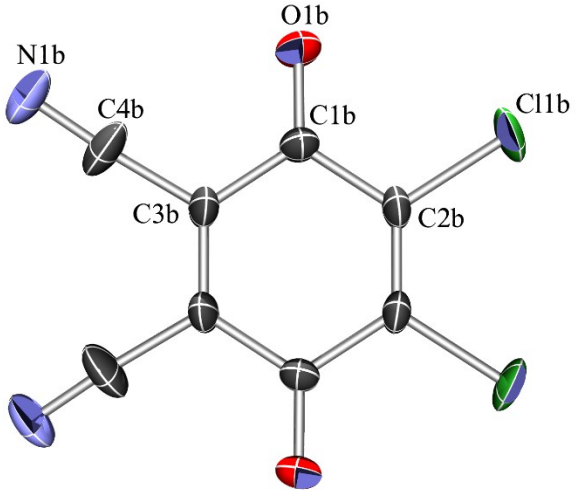

b)

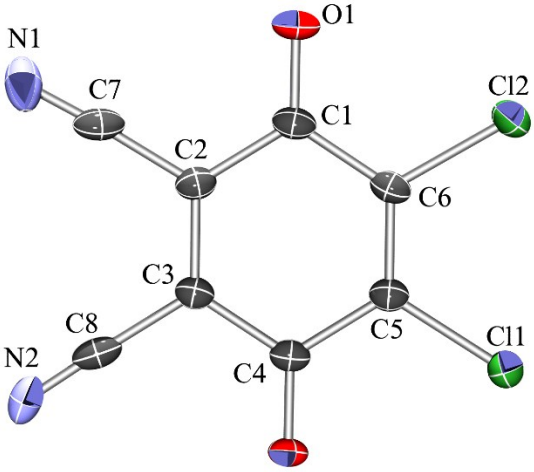

c)

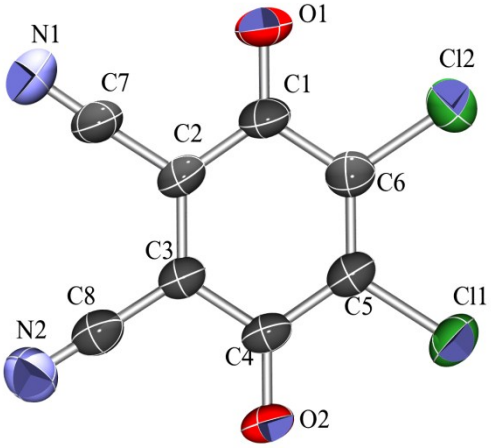

d)

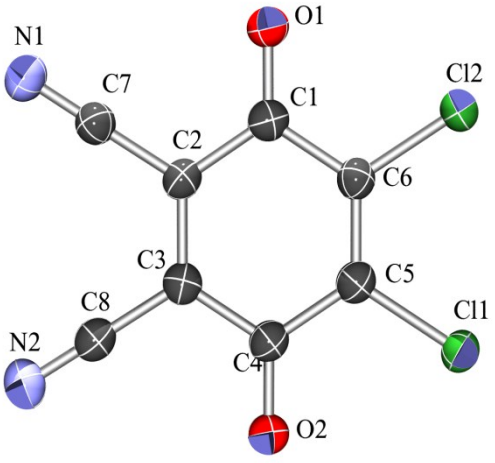

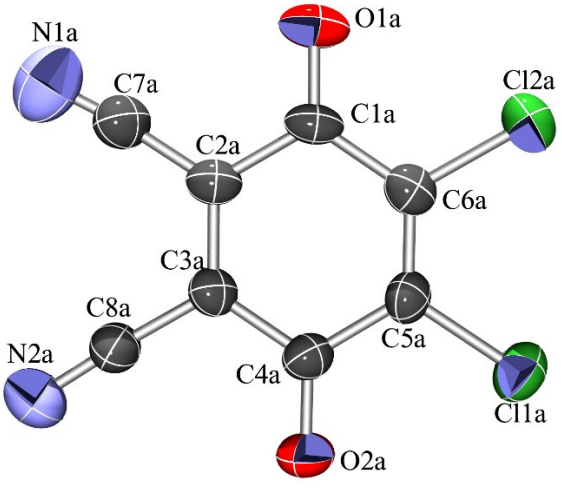

e) f)

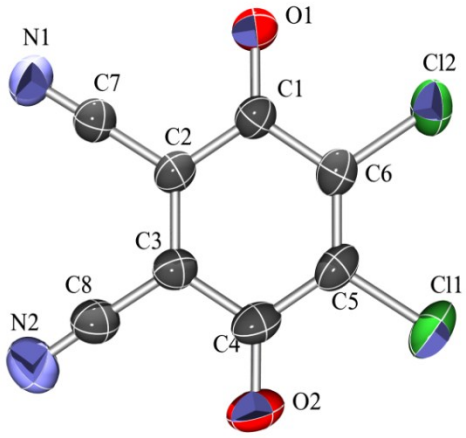

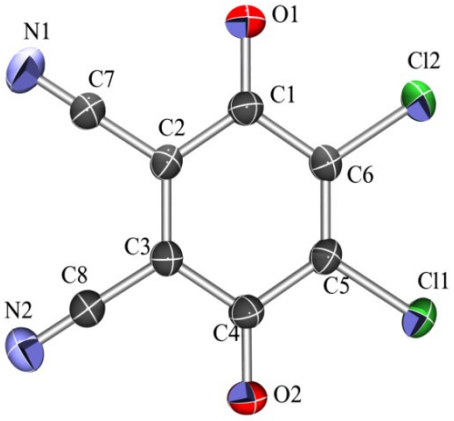

g) h)

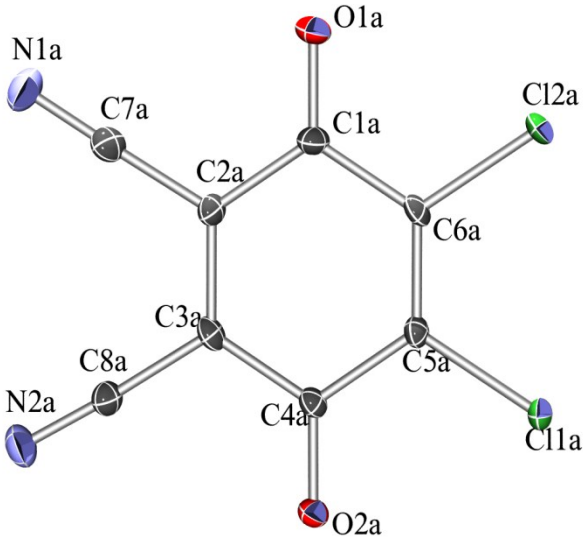

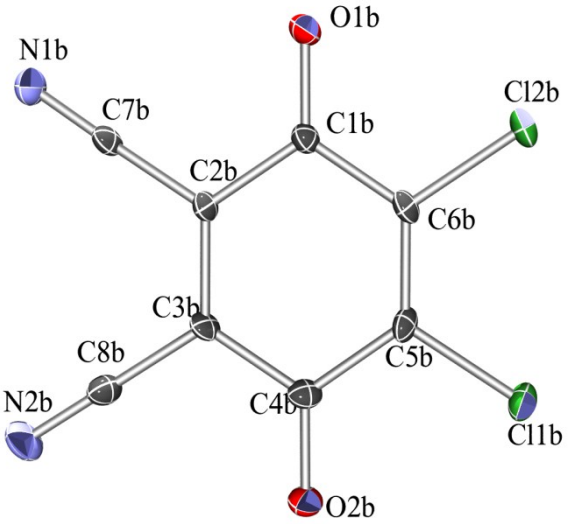

i)

Figure S1 ORTEP-3 drawing of DDQ radical anion with atom numbering scheme in a) **1**, b) **2**-equidistant, c) **2**-dimers, d) **3**, e) **4**, f) **5**, g) **6**, h) **8** and i) two symmetry independent anions in **7**. Displacement ellipsoids are drawn for the probability of 50%; only the major component of the disorder is shown for **2**-equidistant and **5**.

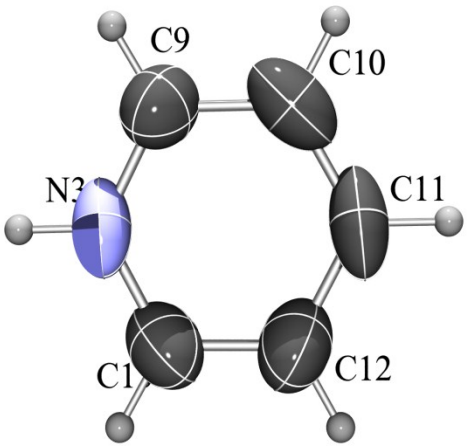
C9
C10
N3
C11
C1
C12

a)

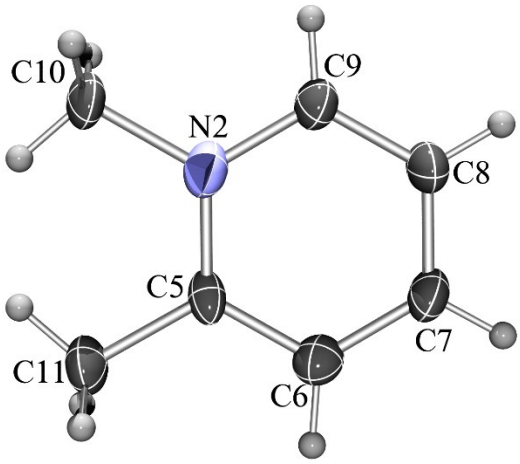
C10
C9
N2
C8
C5
C7
C11
C6

b)

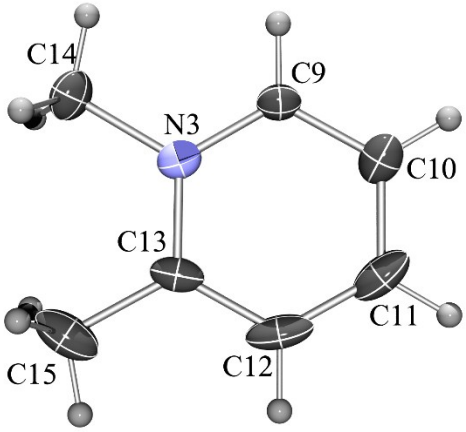
C14
C9
N3
C10
C13
C11
C15
C12

c)

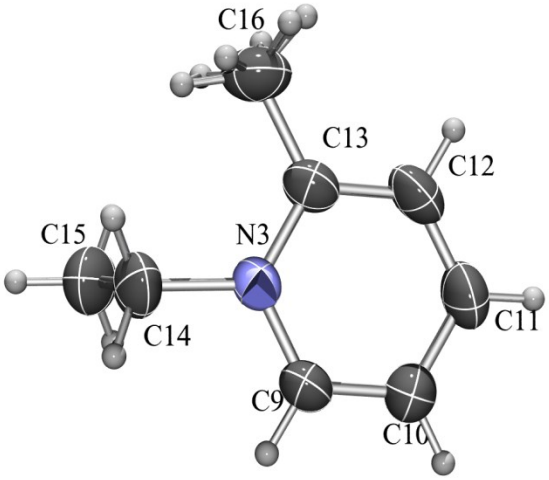
C16
C13
C12
C15
N3
C14
C11
C9
C10

d)

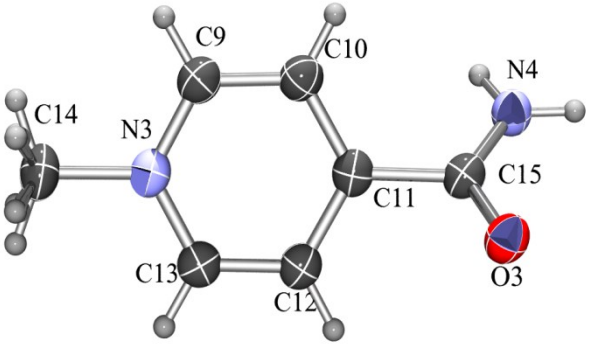
C9
C10
N4
C14
N3
C15
C11
O3
C13
C12

e)

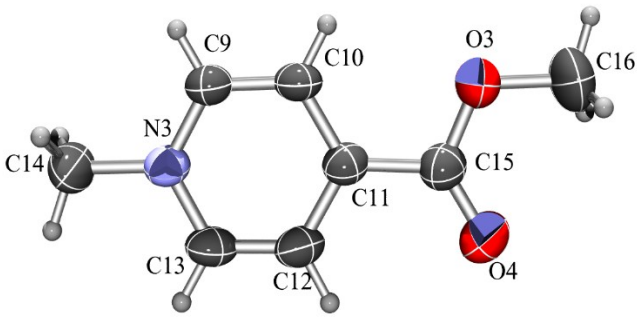
C9
C10
O3
C16
N3
C14
C15
C11
C13
C12
O4

f)

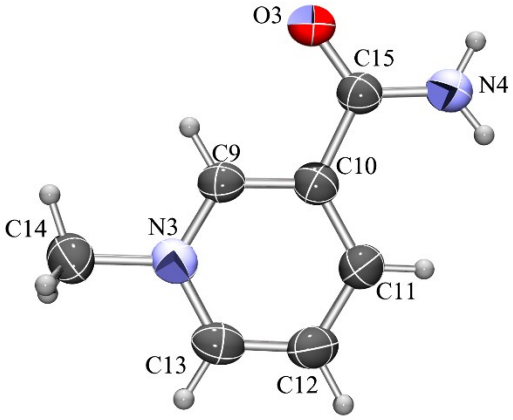
O3
C15
N4
C9
C10
C14
N3
C11
C13
C12

g)

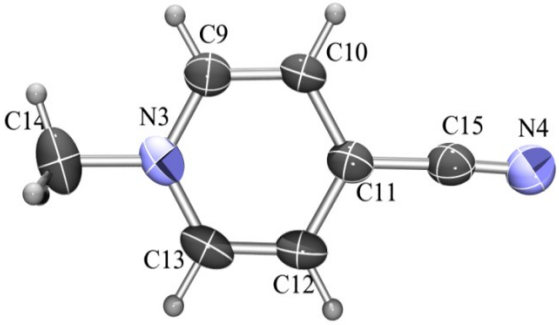
C9
C10
C14
N3
C15
N4
C11
C13
C12

h)

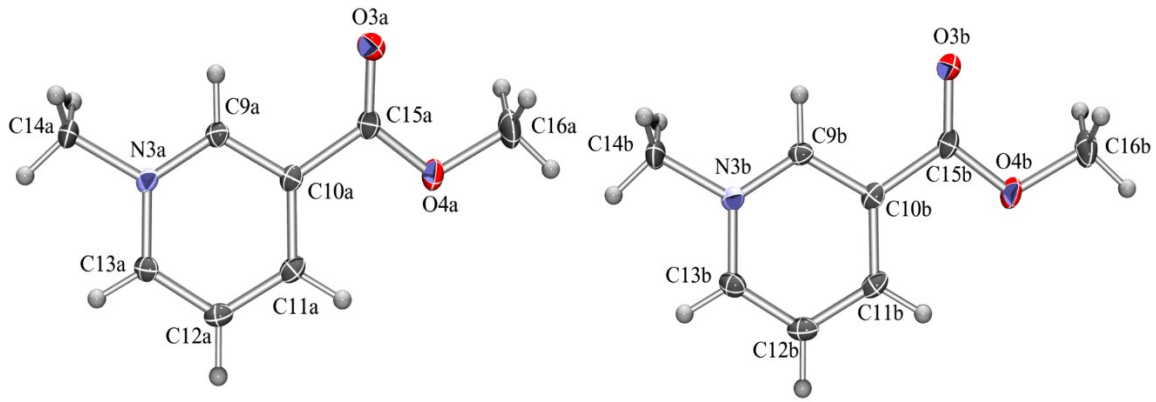

i)

Figure S2 ORTEP-3 drawings of cations: a) pyridinium from **1**, b) *N*-methyl-2-methylpyridinium from **2**-equidistant, c) *N*-methyl-2-methylpyridinium from **2**-dimers, d) *N*-ethyl-2-methylpyridinium from **3**, e) *N*-methyl-4-amidopyridinium from **4**, f) *N*-methyl-4-carboxymethylpyridinium from **5**, g) *N*-methyl-3-amidopyridinium from **6**, h) *N*-methyl-4-cyanopyridinium from **8**, and i) two symmetry-independent *N*-methyl-3-carboxymethylpyridinium cations from **7**. Displacement ellipsoids are drawn for the probability of 50 % and hydrogen atoms are shown as spheres of arbitrary radii.

S2 Geometry of the DDQ radical anion

Table S1 Geometric parameters of DDQ radical anions (Å, °). Compounds **2**-equidistant and **5** have been omitted due to disorder and poor data, respectively.

	1	**2**-dimers	**3**	**4**	**6**	**7** A	**7** B	**8**
C1-O1	1.238(3)	1.243(3)	1.242(2)	1.239(3)	1.245(3)	1.242(3)	1.245(3)	1.2418(15)
C4-O2	1.253(3)	1.241(3)	1.245(2)	1.248(3)	1.245(3)	1.245(3)	1.239(3)	1.2379(16)
C1-C2	1.454(4)	1.458(3)	1.444(3)	1.452(4)	1.449(3)	1.444(3)	1.453(3)	1.4522(17)
C2-C3	1.374(3)	1.388(3)	1.383(2)	1.391(3)	1.387(3)	1.390(3)	1.383(3)	1.3870(17)
C3-C4	1.439(3)	1.446(3)	1.445(2)	1.447(3)	1.452(3)	1.443(3)	1.450(3)	1.4552(17)
C4-C5	1.467(4)	1.470(3)	1.469(3)	1.462(4)	1.462(4)	1.472(3)	1.470(3)	1.4650(17)
C5-C6	1.357(3)	1.363(3)	1.361(3)	1.373(4)	1.359(3)	1.360(3)	1.362(3)	1.3548(17)
C6-C1	1.470(4)	1.461(3)	1.461(3)	1.467(3)	1.465(3)	1.469(3)	1.463(3)	1.4693(17)
C2-C7	1.432(4)	1.434(3)	1.431(3)	1.433(3)	1.433(3)	1.431(4)	1.436(4)	1.4322(17)
C3-C8	1.439(4)	1.445(3)	1.429(3)	1.440(4)	1.427(4)	1.438(3)	1.438(3)	1.4324(17)
C7-N1	1.135(5)	1.083(3)	1.128(3)	1.150(3)	1.135(3)	1.155(4)	1.154(3)	1.1407(17)
C8-N2	1.134(4)	1.062(3)	1.109(3)	1.143(4)	1.141(4)	1.149(3)	1.150(3)	1.1469(18)
C5-Cl1	1.719(2)	1.737(2)	1.723(2)	1.726(2)	1.717(2)	1.720(2)	1.722(2)	1.7145(12)
C6-Cl2	1.715(3)	1.738(2)	1.724(2)	1.711(3)	1.723(2)	1.716(2)	1.719(2)	1.7147(13)
τ	3.9	2.8	4.2	2.5	3.0	3.8	2.8	3.9

S3 Data on crystal packings

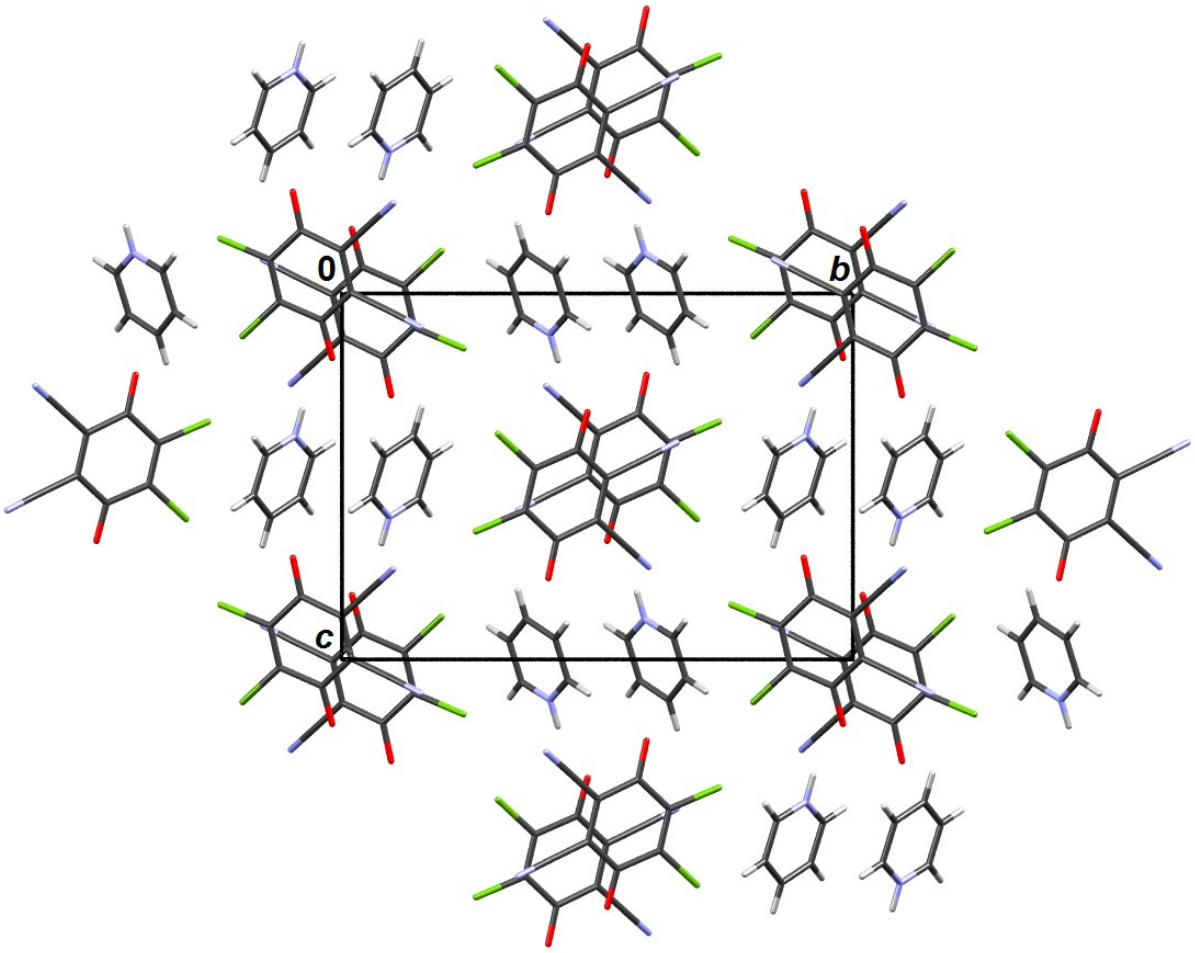

Figure S3 Crystal packing of **1** viewed in the direction [100].

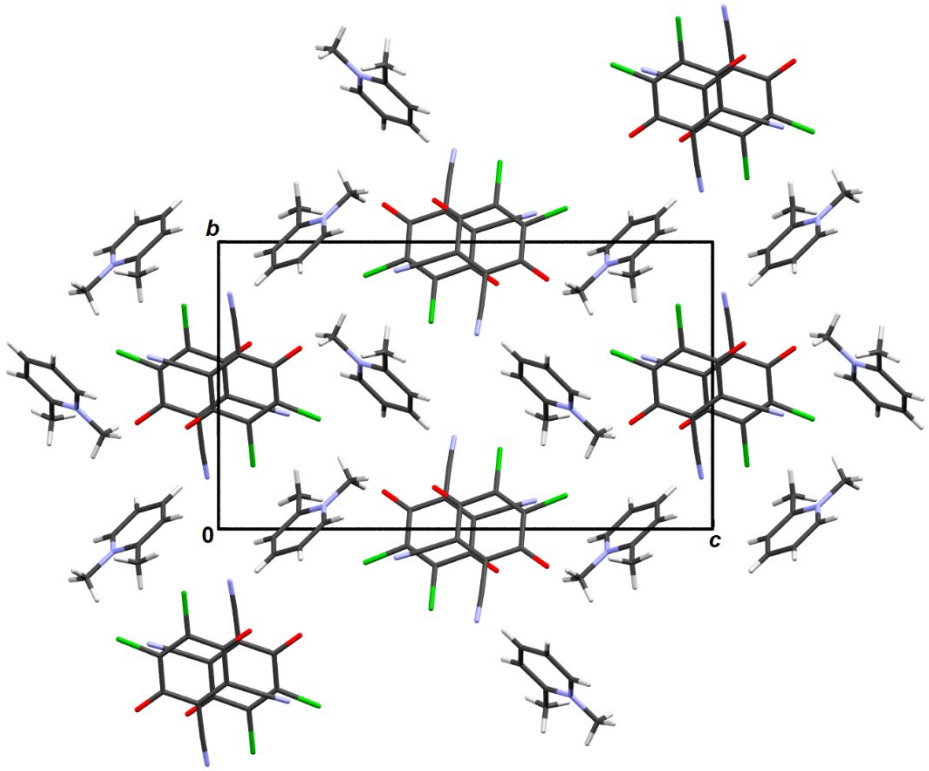

Figure S4 Crystal packing of **2-dimers** viewed in the direction [100].

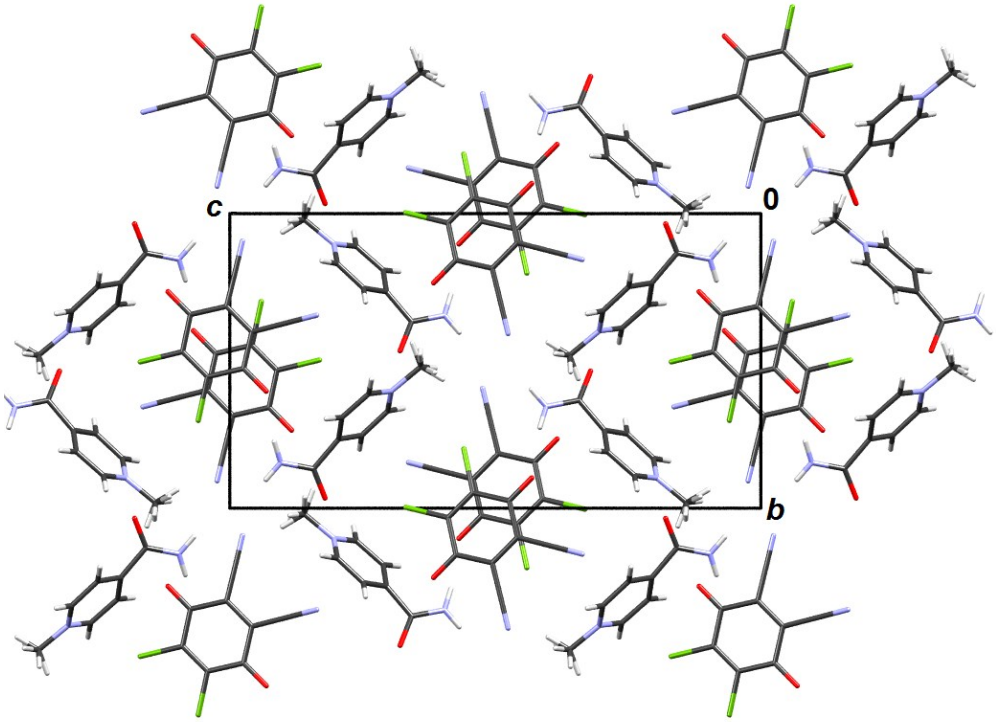

Figure S5 Crystal packing of **4** viewed in the direction [100].

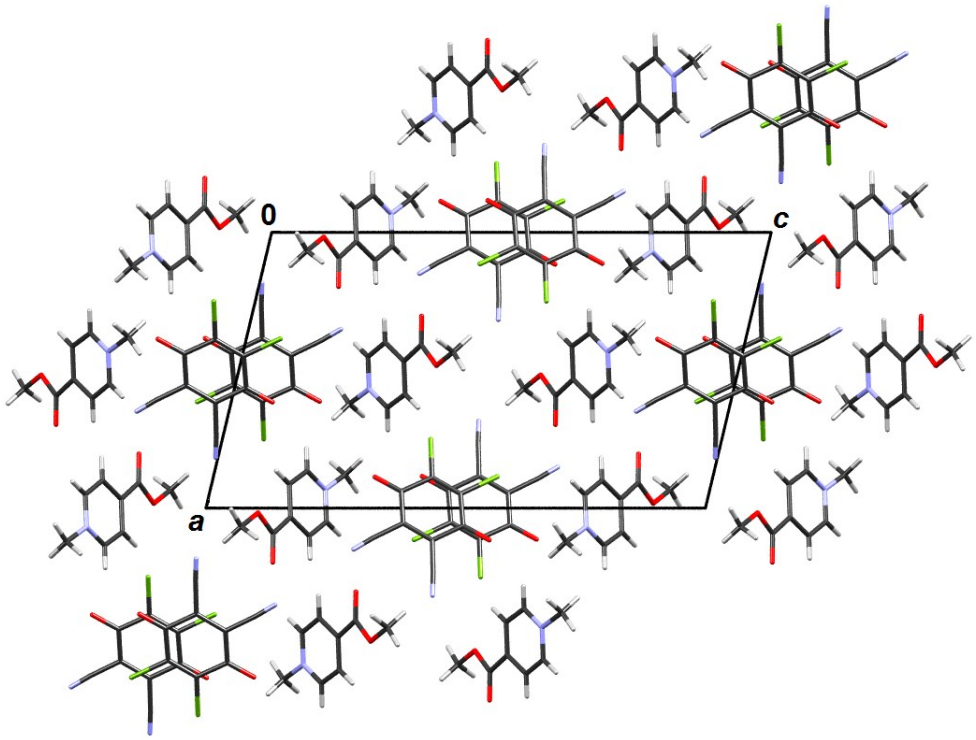

Figure S6 Crystal packing of **5** viewed in the direction [010].

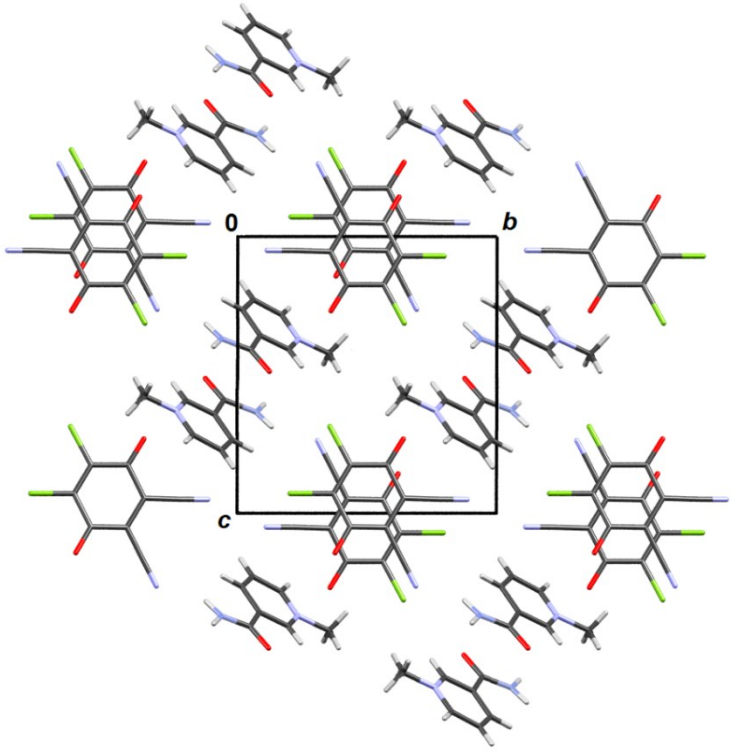

Figure S7 Crystal packing of **6** viewed in the direction [100].

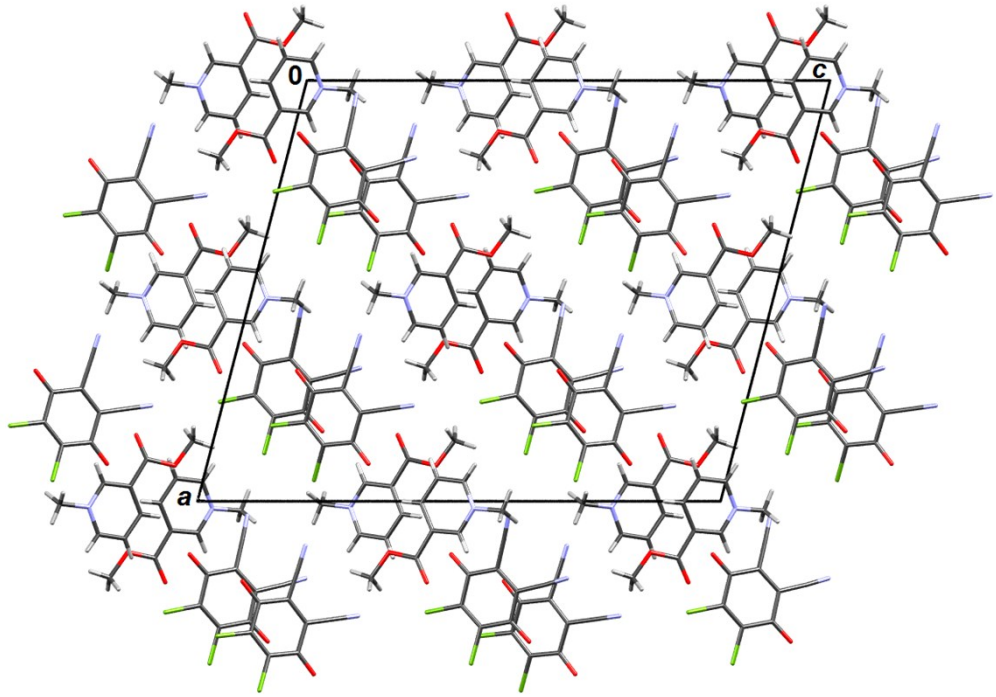

Figure S8 Crystal packing of **7** viewed in the direction [010].

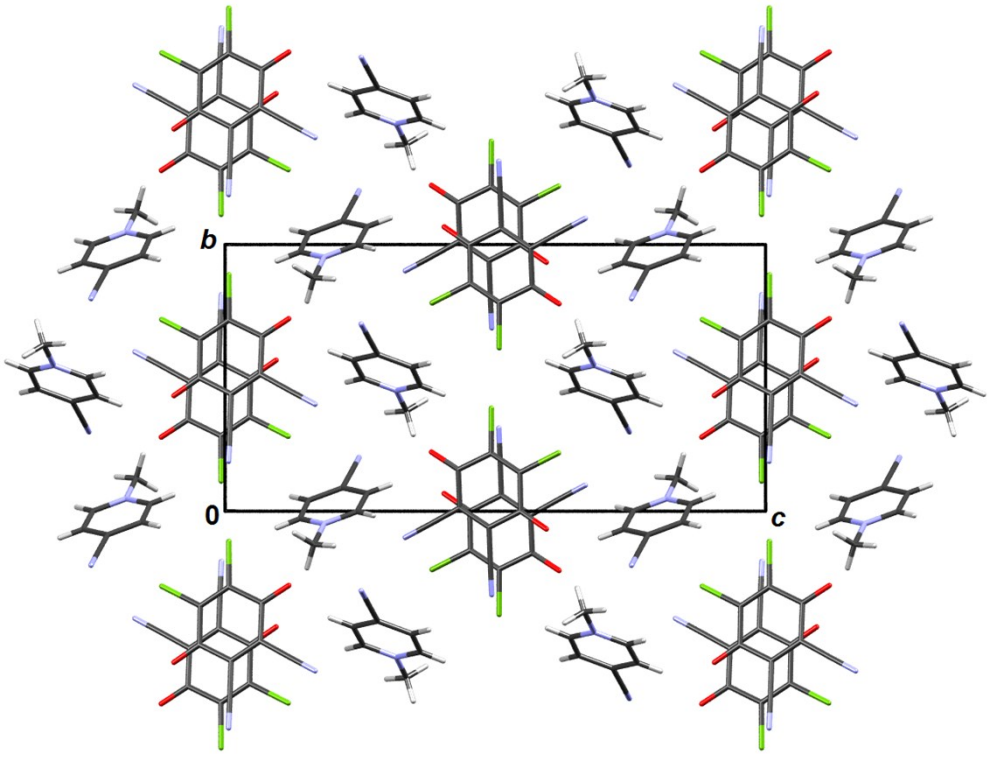

Figure S9 Crystal packing of **8** viewed in the direction [100].

S4 Details on electrical measurements

Axes of all crystals were checked on a diffractometer: unit cell and orientation matrix were found, and then direction of the crystallographic axes were found using the tool for indexing faces (simply by defining faces {100}, {010} and {001}). In all compounds the direction of stacking corresponded to the longest axis of the crystal (Figs. S10-S17). The electrical contacts were made by application of silver paste to opposite ends of rod-like crystals (Fig. S18). For electrical measurements we used the largest crystals in our samples, which were typically about 0.5 mm long and 0.1 mm thick.

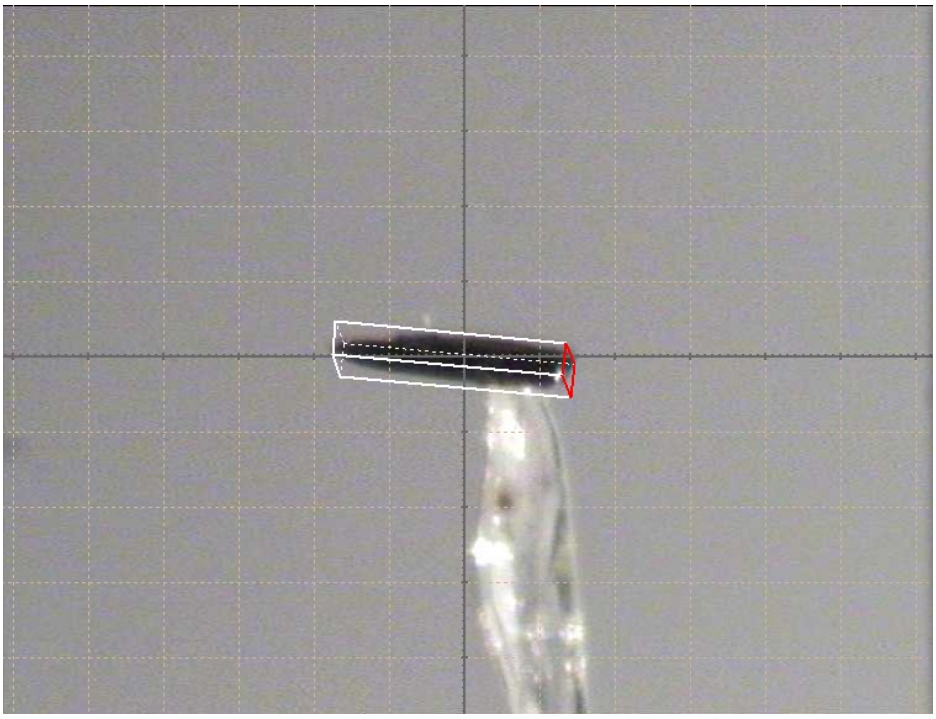

Figure S10 Crystal of **2**-equidistant with crystallographic axes indicated by defining fictive faces {100}, {010} and {001}. Direction of stacking is the longest axis, [100], so the (100) face is highlighted in red.

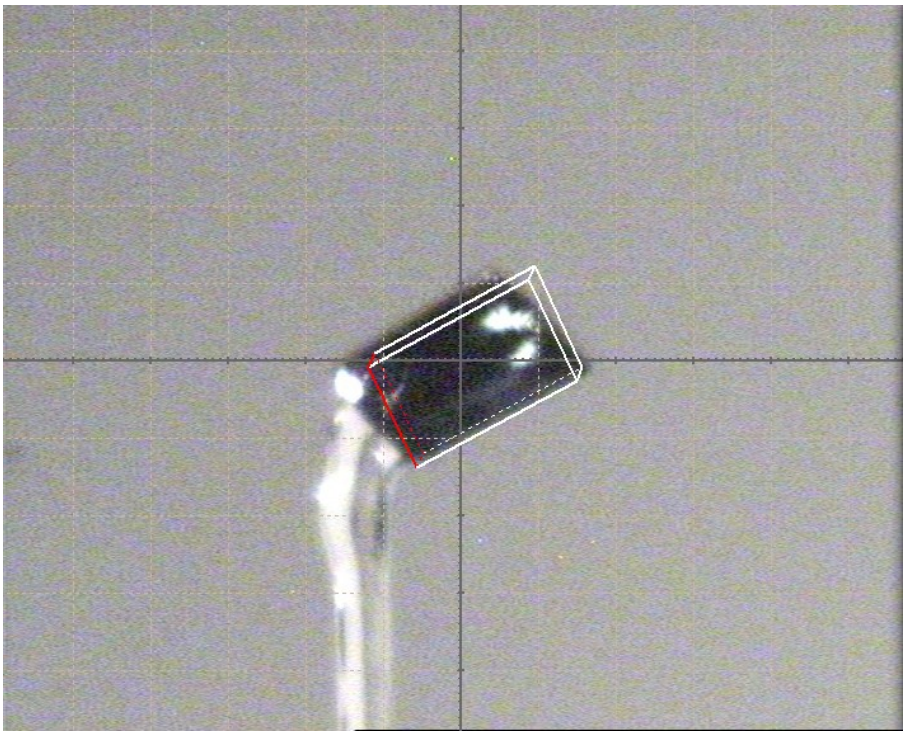

Figure S11 Crystal of **2**-dimers with crystallographic axes indicated by deifning fictive faces {100}, {010} and {001}. Direction of stacking is the longest axis, [100], so the (100) face is highlighted in red.

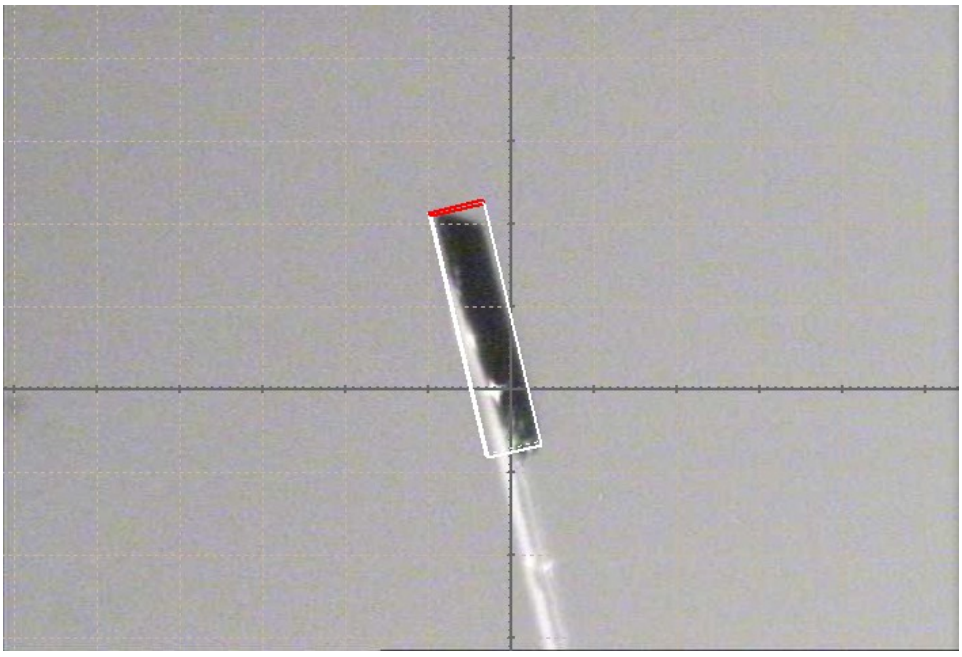

Figure S12 Crystal of **3** with crystallographic axes indicated by defining fictive faces {100}, {010} and {001}. Direction of stacking is the longest axis, [001], so the (001) face is highlighted in red.

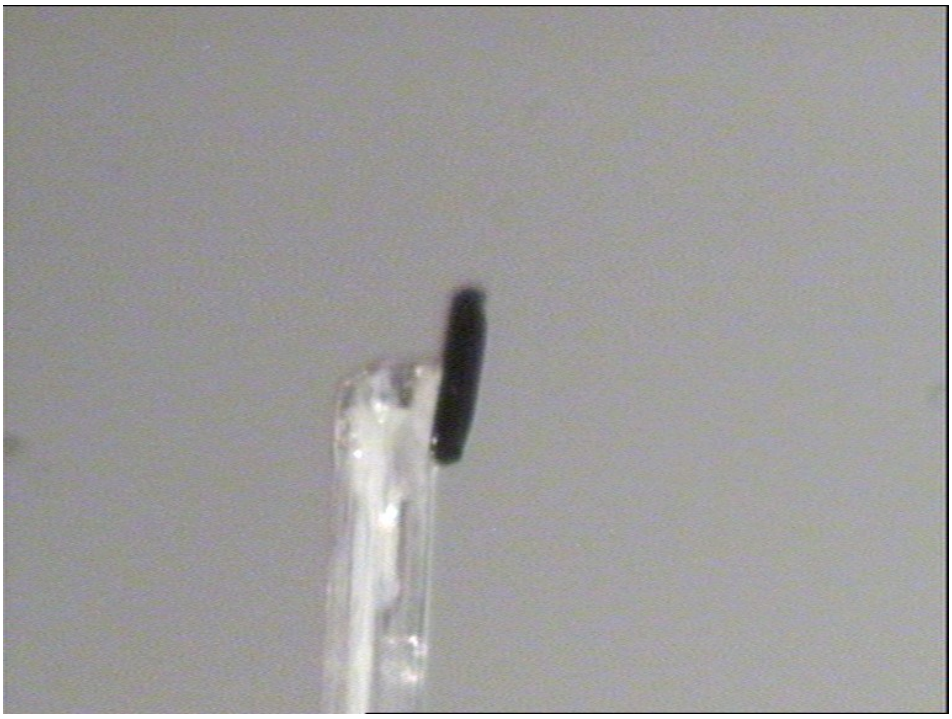

Figure S13 Crystal of **4**. The raw data were unfortunately lost due to a malfunction of a hard drive; however it is reasonable to assume that the longest axis of the crystal corresponds to the direction [100], which is the direction of stacking.

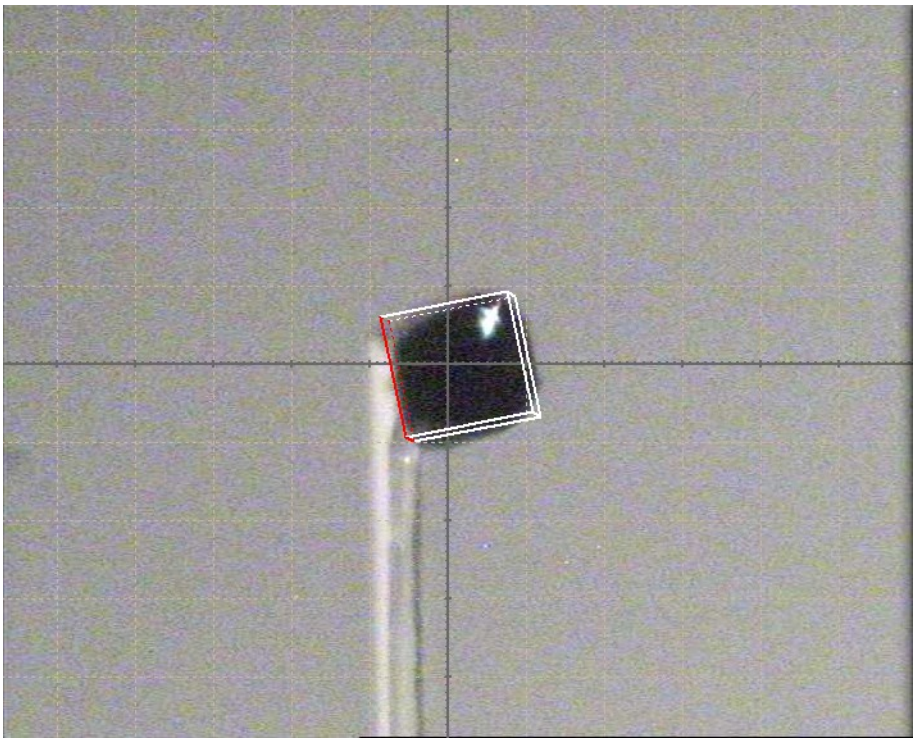

Figure S14 Crystal of **5** with crystallographic axes indicated by defining fictive faces {100}, {010} and {001}. Direction of stacking is [010], so the (010) face is highlighted in red.

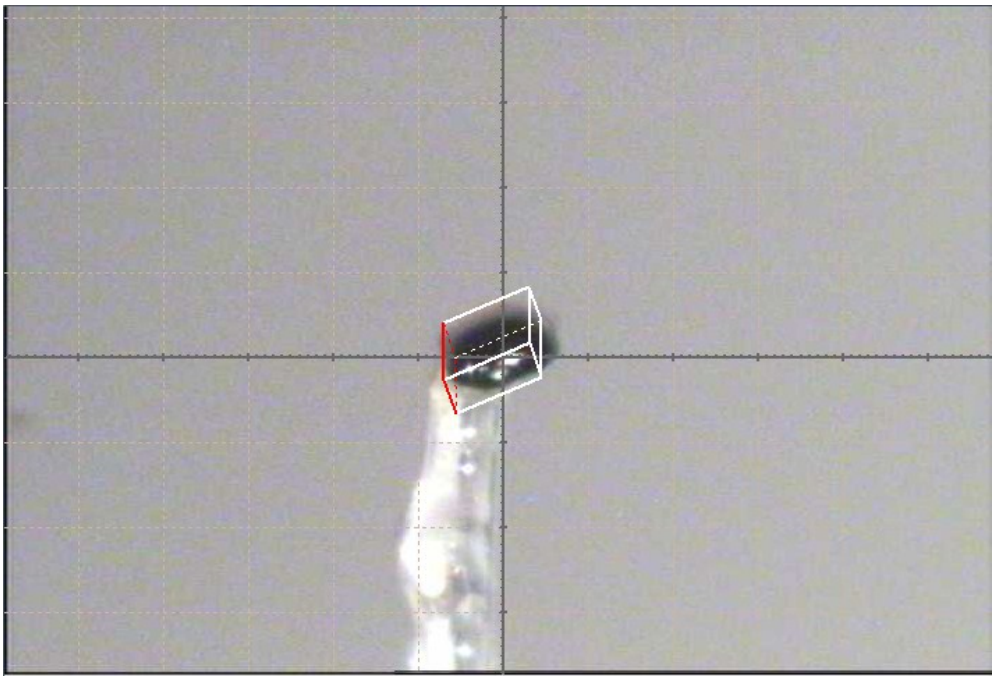

Figure S15 Crystal of **6** with crystallographic axes indicated by defining fictive faces {100}, {010} and {001}. Direction of stacking is the longest axis, [100], so the (100) face is highlighted in red.

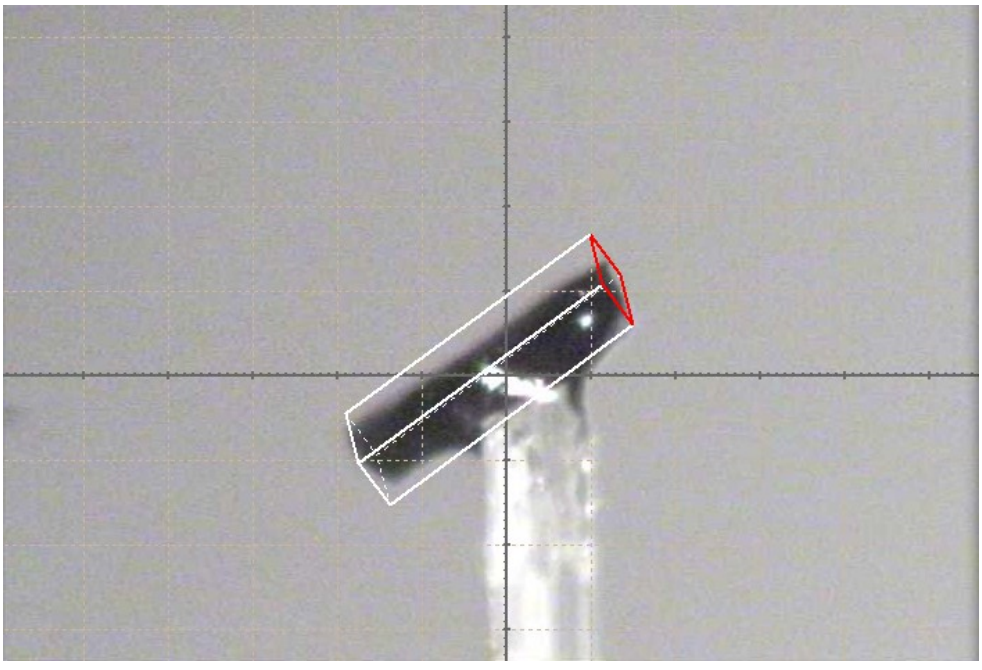

Figure S16 Crystal of **7** with crystallographic axes indicated by defining fictive faces {100}, {010} and {001}. Direction of stacking is the longest axis, [010], so the (010) face is highlighted in red.

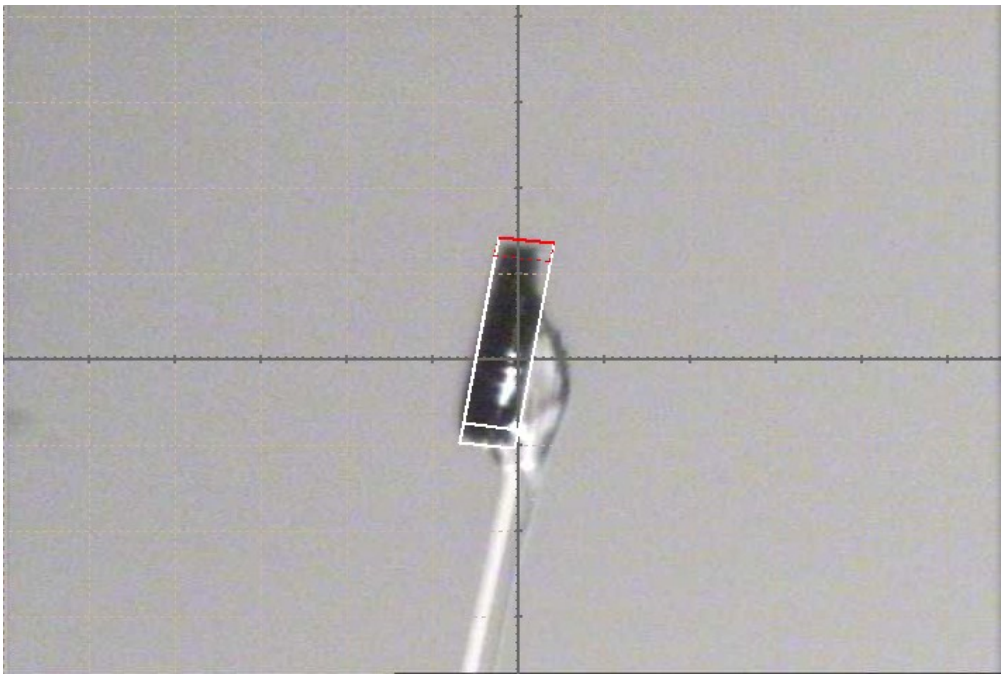

Figure S17 Crystal of **8** with crystallographic axes indicated by defining fictive faces {100}, {010} and {001}. Direction of stacking is the longest axis, [100], so the (100) face is highlighted in red.

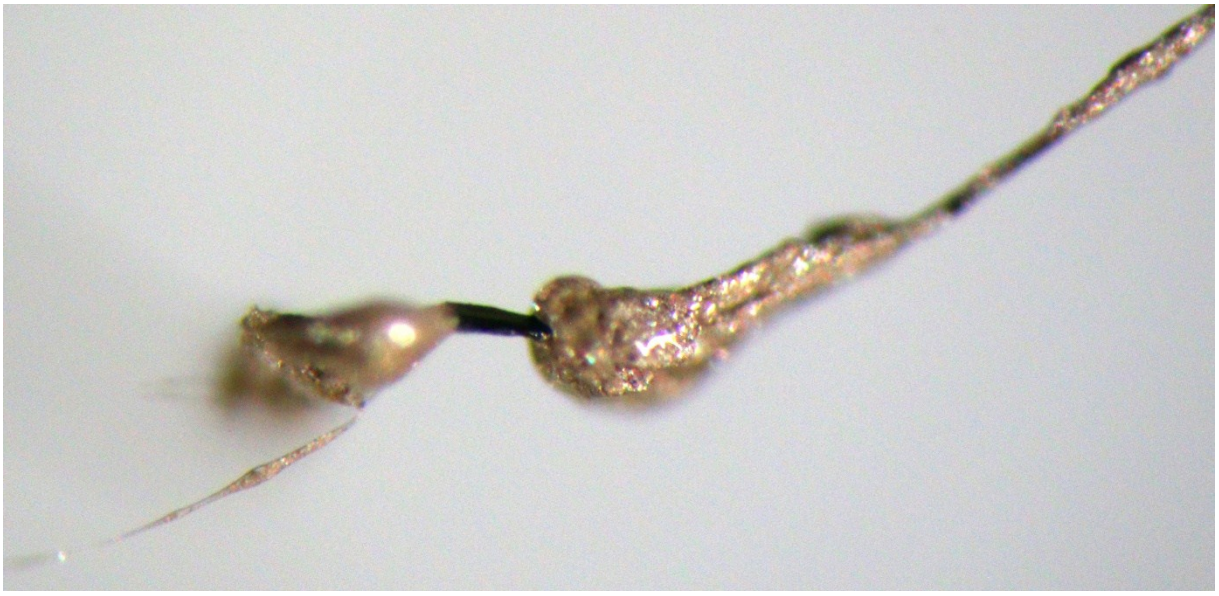

Figure S18 A photograph of a small crystal of **9** (*ca*. 0.25 mm long) with electrical contacts applied to faces {100}.

S5 Cartesian coordinates of the converged geometries and the corresponding absolute energies (in Hartrees).

Cis-(parallel)-DDQ_2^{2-} dimer at UM05-2X/6-311G(d,p), -2970.59602664 Hartrees.

Cl	-0.155937000000	-2.446349000000	-1.759686000000
Cl	-2.914411000000	-2.670167000000	-0.182980000000
O	-3.930087000000	-0.075337000000	0.651752000000
O	0.809229000000	0.297995000000	-1.944823000000
N	-3.614207000000	3.389092000000	0.334442000000
N	-0.212957000000	3.662774000000	-1.843236000000
C	-2.851785000000	0.022481000000	0.083860000000
C	-2.230830000000	1.297829000000	-0.252644000000
C	-1.034720000000	1.392298000000	-0.941427000000
C	-0.275565000000	0.225328000000	-1.366735000000
C	-0.942640000000	-1.061088000000	-1.089925000000
C	-2.121173000000	-1.152077000000	-0.430813000000
C	-2.981087000000	2.460493000000	0.090304000000
C	-0.560326000000	2.652175000000	-1.420495000000
Cl	2.940234000000	-2.643047000000	0.183737000000
Cl	0.180122000000	-2.446815000000	1.757640000000
O	-0.813740000000	0.288511000000	1.941609000000
O	3.932987000000	-0.037859000000	-0.648846000000
N	0.173777000000	3.662724000000	1.840392000000
N	3.582366000000	3.424192000000	-0.328362000000
C	0.272623000000	0.226483000000	1.364834000000
C	1.020797000000	1.400681000000	0.940762000000
C	2.219180000000	1.318379000000	0.254022000000
C	2.852934000000	0.049453000000	-0.082390000000
C	2.132384000000	-1.132206000000	0.430152000000
C	0.952487000000	-1.052919000000	1.088513000000
C	0.532470000000	2.655712000000	1.418599000000
C	2.958570000000	2.488722000000	-0.086329000000

Trans-(antiparallel)-DDQ_2^{2-} dimer at UM05-2X/6-311G(d,p), -2970.60392538 Hartrees.

Cl	-1.653626000000	-2.266068000000	1.563929000000
Cl	-3.992142000000	-0.966471000000	-0.163451000000
O	-3.542910000000	1.866108000000	-0.690670000000
O	0.511169000000	-0.391894000000	2.095851000000
N	-1.450324000000	4.629066000000	-0.150424000000
N	1.467161000000	2.995758000000	2.067853000000
C	-2.608513000000	1.355655000000	-0.077780000000
C	-1.456000000000	2.108225000000	0.379350000000
C	-0.431277000000	1.536019000000	1.117228000000
C	-0.411893000000	0.132135000000	1.471126000000
C	-1.603123000000	-0.621638000000	1.041004000000
C	-2.604130000000	-0.062214000000	0.320579000000

C	-1.451244000000	3.500694000000	0.073479000000
C	0.636026000000	2.332063000000	1.630799000000
Cl	1.652004000000	2.265829000000	-1.564920000000
Cl	3.991253000000	0.968099000000	0.162839000000
O	3.542943000000	-1.864143000000	0.692360000000
O	-0.511048000000	0.389713000000	-2.097764000000
N	1.452037000000	-4.628669000000	0.152449000000
N	-1.464911000000	-2.998277000000	-2.068367000000
C	2.608493000000	-1.354557000000	0.078853000000
C	1.456532000000	-2.108023000000	-0.378256000000
C	0.431865000000	-1.536855000000	-1.116998000000
C	0.411746000000	-0.133104000000	-1.471629000000
C	1.602329000000	0.621577000000	-1.041354000000
C	2.603577000000	0.063008000000	-0.320564000000
C	1.452463000000	-3.500360000000	-0.071771000000
C	-0.634563000000	-2.333799000000	-1.630993000000